

## University of Groningen

### Integrative omics to understand human immune variation

Aguirre Gamboa, Raul

DOI:  
[10.33612/diss.98324185](https://doi.org/10.33612/diss.98324185)

**IMPORTANT NOTE:** You are advised to consult the publisher's version (publisher's PDF) if you wish to cite from it. Please check the document version below.

*Document Version*  
Publisher's PDF, also known as Version of record

*Publication date:*  
2019

[Link to publication in University of Groningen/UMCG research database](#)

*Citation for published version (APA):*  
Aguirre Gamboa, R. (2019). *Integrative omics to understand human immune variation*. [Thesis fully internal (DIV), University of Groningen]. University of Groningen. <https://doi.org/10.33612/diss.98324185>

#### Copyright

Other than for strictly personal use, it is not permitted to download or to forward/distribute the text or part of it without the consent of the author(s) and/or copyright holder(s), unless the work is under an open content license (like Creative Commons).

The publication may also be distributed here under the terms of Article 25fa of the Dutch Copyright Act, indicated by the "Taverne" license. More information can be found on the University of Groningen website: <https://www.rug.nl/library/open-access/self-archiving-pure/taverne-amendment>.

#### Take-down policy

If you believe that this document breaches copyright please contact us providing details, and we will remove access to the work immediately and investigate your claim.

Downloaded from the University of Groningen/UMCG research database (Pure): <http://www.rug.nl/research/portal>. For technical reasons the number of authors shown on this cover page is limited to 10 maximum.

5

---

6

---

7

General introduction and aim outline of the thesis

Differential effects of environmental and Genetic factors on T and B cell Immune traits.

A functional genomics approach to understand variation in cytokine production in humans.

Integration of multi-omics data and deep phenotyping enables prediction of cytokine responses.

Deconvolution of bulk blood eQTL effects into immune cell subpopulations.

Tissue alarmins and adaptive cytokine induce dynamic and distinct transcriptional responses in tissue-resident intraepithelial cytotoxic T lymphocytes

Discussion and perspectives

# Tissue alarmins and adaptive cytokine induce dynamic and distinct transcriptional responses in tissue-resident intraepithelial cytotoxic T lymphocytes

## AUTHORS

Maria Magdalena Zorro<sup>1†</sup>, Raul Aguirre-Gamboa<sup>1†</sup>, Toufic Mayassi<sup>2,3</sup>, Cezary Ciszewski<sup>2</sup>, Sebo Withoff<sup>1</sup>, Yang Li<sup>1,4</sup>, Cisca Wijmenga<sup>1,5</sup>, Bana Jabri<sup>2,3##\*</sup>, Iris Jonkers<sup>1,5##\*</sup>

† These authors contributed equally

# These authors contributed equally

\* Corresponding Author

## AFFILIATIONS

1 Department of Genetics, University Medical Center Groningen, University of Groningen, Groningen, the Netherlands

2 Department of Medicine, University of Chicago, Chicago, USA

3 Committee on Immunology, University of Chicago, Chicago, USA

4 Department of Internal Medicine and Radboud Center for Infectious Diseases (RCI), Radboud University Medical Center, Nijmegen, the Netherlands

5 Department of Immunology, K.G. Jebsen Coeliac Disease Research Centre, University of Oslo, Oslo, Norway

Corresponding Author

i.h.jonkers@umcg.nl

bjabri@bsd.uchicago.edu

## ABSTRACT

The effects of tissue alarmins, like interleukin(IL)-15 and interferon beta (IFN $\beta$ ), and cytokines, like IL-21, on the intraepithelial cytotoxic T lymphocytes (IE-CTLs) that can mediate tissue destruction in patients with immune disorders is poorly understood. Our analysis of the dynamics of transcriptomic and epigenomic profiles in primary IE-CTLs shows massive and distinct temporal transcriptional changes in response to tissue alarmins, while the impact of IL-21 was limited. Only anti-viral pathways were induced in response to all three stimuli. Interestingly, the dynamically differentially expressed genes, particularly genes involved in the IFN pathway, are enriched in autoimmune disease risk loci. Changes in gene expression were mostly independent of changes in H3K27ac, suggesting that other regulatory mechanisms may contribute to the robust transcriptional response. Together these results provide new insights into the mechanisms that fuel activation of tissue-resident CTLs under conditions that emulate the inflammatory environment in patients with immune-mediated diseases.

**Key words:** autoimmune disease, cytotoxic T lymphocytes, intraepithelial lymphocytes, IFN $\beta$ , IL-15, IL-21, tissue-resident lymphocytes

## INTRODUCTION

Tissue-resident cytotoxic T lymphocytes (CTLs) have been shown to play a critical role in mediating tissue destruction in organ-specific autoimmune disorders(Jabri and Abadie, no date; Jabri and Meresse, 2006). Understanding the molecular mechanisms that underlie CTL activation within the tissue environment will help identify new therapeutic strategies. CTL differentiation, activation and function are greatly influenced by the tissue microenvironment, where they sense and respond to microbial products, cytokines and alarmins(Sheridan and Lefrançois, 2010; Fan and Rudensky, 2016). Specifically, chronic production of innate immune or epithelial cell-derived cytokines (e.g. IFN $\beta$  and IL-15, also referred to as tissue alarmins) and T-cell-de-

rived cytokines (e.g. IL-21) have been shown to modulate the expansion and/or effector functions of CTLs and to contribute to the development of tissue-specific immune-mediated disorders including celiac disease (CeD), rheumatoid arthritis (RA), inflammatory bowel disease (IBD) and type 1 diabetes (T1D)(Sheridan and Lefrançois, 2010; Moudgil and Choubey, 2011; Yuan et al., 2011; Ciechomska and Skalska, 2018). However, because it is difficult to collect materials from human tissues from the site of disease, our understanding of the contribution of tissue-derived alarmins versus the role of cytokines produced by antigen-specific T cells in the development of autoimmune disorders and activation of tissue-resident CTLs remains poorly understood(Raine et al., 2015; Hoytema van Konijnenburg and Mucida, 2017). Intraepithelial CTL (IE-CTLs) are tissue-resident cytotoxic T lymphocytes that are located in between intestinal epithelial cells. IE-CTLs protect against infection directly, by killing infected cells, and indirectly, by promoting the immune response via production of cytokines such as IFN $\gamma$ (Hoytema van Konijnenburg and Mucida, 2017; Mayassi and Jabri, 2018). They are also the key effector cell type in mediating the tissue destruction central to the pathogenesis of some autoimmune diseases, including CeD and T1D(Jabri et al., 2000; Tsai, Shameli and Santamaria, 2008; Jabri and Sollid, 2009). Type-1 IFNs (IFN-1), IL-15 and IL-21 are all upregulated in active CeD, a complex T-cell-mediated enteropathy with an autoimmune component that is induced by dietary gluten and characterized by the presence of villous atrophy in the intestinal mucosa(Jabri and Sollid, 2009). Interestingly, IL-15 and IL-21 are absent in patients who have lost tolerance to dietary gluten but who have not yet developed villous atrophy (a condition called “potential CeD”), indicating that these alarmins may play a crucial part in tissue destruction(Sperandeo et al., 2011; Setty et al., 2015; Borrelli et al., 2016). IFN $\beta$ (Di Sabatino et al., 2007) and IL-15(Jabri et al., 2000; Mention et al., 2003; Di Sabatino et al., 2006) are upregulated in intestinal epithelial cells and antigen presenting cells(Di Sabatino et al., 2006, 2007), and IL-21 is produced by gluten-specific CD4 $^{+}$  T cells(Bodd et al., 2010), but the effect of IFN $\beta$ , IL-15 and IL-21 in the activation of IE-CTLs remains to be determined.

Here we report the first comparative characterization of the dynamics of

transcriptomic and epigenetic changes in primary-tissue-resident IE-CTL lines upon exposure to tissue-derived alarmins and adaptive cytokines involved in disease pathophysiology. We stimulated CD8<sup>+</sup> TCR $\alpha\beta$  IE-CTLs isolated from intestinal biopsies with IFN-1 (IFN $\beta$ ), IL-15 and IL-21 at multiple time points. This allowed us to characterize the overall changes in gene expression and the pathways affected under these different inflammatory conditions. We analyzed genome-wide H3K27ac signatures to identify epigenetic changes critical for the modulation of transcriptional responses to these cytokines.

## Material and methods

**Human subjects:** Control individuals who were undergoing endoscopies and biopsies for functional intestinal disorders of non-celiac origin and CeD patients who were diagnosed based on the presence of elevated anti-transglutaminase antibodies in serum, expression of HLA DQ2 or DQ8, presence of increased IE-CTLs, partial or total duodenal villous atrophy, crypt hyperplasia on duodenal biopsy and clinical response to a gluten free diet. All subjects gave written informed consent and all protocols were approved by the University of Chicago Institutional Review Board.

**IE-CTL cultures:** TCR $\alpha\beta$ <sup>+</sup> CD8<sup>+</sup> short-term IE-CTL cell lines derived from 4-6 duodenal biopsies from CeD patients (n=4) or healthy control individuals (n=4) were generated as previously described (Jabri et al., 2000; Roberts et al., 2001). Briefly, cells from the intraepithelial lymphocyte compartment were isolated via 1 hr of mechanical disruption in media containing 1% dialyzed fetal bovine serum (Biowest), 2mM EDTA (Corning) and 1.5mM MgCl<sub>2</sub> (Thermo Fisher Scientific). Up to 10,000 cells expressing both TCR $\alpha\beta$  (IP26, BioLegend) and CD8 $\alpha$  (RPAT-8, BioLegend) were collected via fluorescence-activated cell sorting (FACS) on a FACS Aria II cell sorter (BD Biosciences) and expanded in vitro with a mixture of irradiated heterologous peripheral blood mononuclear cells (from 2 donors) and EBV (Epstein Barr virus) transformed B cells in RPMI 1640 (GIBCO) medium supplemented with 1  $\mu$ g/ml PHA-L (Calbiochem) and 10% human serum albumin (Atlanta Biologicals)



and maintained with 100 units/ml IL-2 (NIH) over the course of expansion. After 14-21 days of expansion, aliquots of cells were frozen for future use to ensure all experiments could be done on the full set of cell lines to avoid experimental batch effects.

**IE-CTL stimulation:** IE-CTLs were thawed and expanded for 12 days as described above. To ascertain cell viability (>80%), cells were analyzed using LIVE/DEAD fixable Aqua Cell Stain Kit (Life Technologies), and cell activation (<10%) was determined by forward and sideward scatter analysis using the LSR Fortessa™ (BD Biosciences) flow cytometer. After 12 days of culture, cells were washed, starved for IL-2 for 48 hrs, and subsequently stimulated for 30 minutes, 3, 4 or 24 hrs with IL-15 (20 ng/ml, Biolegend, cat 570304), IL-21 (3 ng/ml, Biolegend, cat 571204) or IFN $\beta$  (300 ng/ml, Pbl Assay science, cat 11410-2). Unstimulated IE-CTLs were included as control. Prior to the assay, the induction of granzyme B (GZMB), IFNG and BCL2 was measured by qPCR, as a proxy for IE-CTL activation (Berard et al., 2003; Pouw et al., 2010) to determine the optimal cytokine concentration to induce stable expression of the proxies. After stimulation for the indicated periods, cells were collected by centrifugation (10 minutes at 400g) and pellets were lysed in buffer RTL of the RNeasy plus mini kit (Qiagen) for subsequent RNA isolation. A fraction of control cells and cells stimulated for 3 hrs with IL-15, IL-21 and IFN $\beta$  were collected for subsequent chromatin immunoprecipitation. Importantly, all IE-CTL lines from controls and CeD patients were generated and cultured using the same protocols. Of note, IE-CTLs are effector memory T cells, and the short-term lines preserve their tissue-resident status as assessed by their CD103+CD69+CD45RO+ and CD62L- phenotype (Meresse et al., 2006).

**RNA sequencing (RNA-seq):** RNA from unstimulated or stimulated IE-CTLs was isolated with the RNeasy plus mini kit (Qiagen). RNA concentration and quality were measured using the Nanodrop 1000 Spectrophotometer (Thermo Scientific) and the high-sensitivity RNA analysis kit (Experion, software version 3.0, Bio-Rad). RNA-seq libraries were prepared from 1 $\mu$ g of total RNA using the Quant seq 3' kit (Lexogen). The libraries were sequenced on the Nextseq500 (Illumina) yielding at least fifteen million sequence reads per

sample. The fastQ files were then trimmed for low quality reads, adaptors and poly-A tails. Trimmed fastQ files were aligned to build a human\_g1k\_v37 ensemble Release 75 reference genome using hisat(Kim, Langmead and Salzberg, 2015) with default settings and sorted using SAMtools(Li et al., 2009). After alignment, gene level quantification was performed by HTSeq-count(Anders, Pyl and Huber, 2015) using default mode=union. A modified Ensembl version 75 gtf file mapping only to the last 5' 500 bps per gene was used as a gene annotation database to prevent counting of reads mapping to intra-genic A-repeats. Differential expression analysis between time points was performed using the DESeq2(Anders and Huber, 2010) package in R. We defined differentially expressed genes as genes with an absolute log2 fold change ( $|\log_2 FC|$ ) >1 and a False Discovery Rate (FDR)  $\leq 0.01$  between untreated controls and cytokine-treated samples. Principal component analysis (PCA) and heatmaps of hierarchical clustering were done using R base functions (v3.4) to identify the most relevant transcriptional and epigenomic profiles. Gene set enrichment analysis (GSEA)(Subramanian et al., 2005) and Reactome pathways(Haw et al., 2011) were used to detect which biological processes and pathways were enriched in the groups of DEGs. Co-expression analysis and enrichment analysis of co-expression networks was performed using Gene Network v2.0 ([www.genenetwork.nl](http://www.genenetwork.nl))(Deelen et al., 2018).

**Chromatin immunoprecipitation and library preparation:** Cell pellets from unstimulated or 3h-stimulated IE-CTLs were cross-linked with 1% formaldehyde at room temperature for 5 min. Nuclei were isolated with the truChIP chromatin shearing kit (Covaris). Chromatin was sheared for 6 minutes by sonication in the S220 sonicator (Covaris; 140 watts, 5% duty factor, 200 CPB). Chromatin immunoprecipitation and ChIP-seq library preparation were performed according to protocols described by the Blueprint consortium (<http://www.blueprint-epigenome.eu>). In brief, 22  $\mu$ l of chromatin was incubated overnight at 4oC with 1  $\mu$ g of H3K27ac antibody (Diagenode, cat C15410196), followed by 1-hour incubation with protein A- and G-coated beads (Invitrogen, Dynabeads. Catalog 1003D and 1004D). The chromatin was reverse crosslinked for 4 hrs at 65oC in the presence of proteinase K

(0.1  $\mu\text{g}/\mu\text{l}$ , Roche, cat 3115887001), then purified using the QIAquick MinElute PCR Purification Kit (Qiagen). The libraries were prepared using the Kapa Hyper Prep Kit (Kapa biosystem). After end repair, tailing and Nexflex adapter ligation (Nextera), the libraries were amplified for 10 cycles, then purified with the QIAquick MinElute PCR Purification Kit. DNA fragments 300 bp in size were purified with LabChip Caliper XT 700 electrophoresis system (Perkin Elmer). Library concentration and fragment size distribution were analyzed using the High sensitivity NGS fragment analysis kit using the Fragment Analyzer (Advanced Analytical). ChIP-seq libraries were sequenced (50 bp single end reads) using the Nextseq500 sequencer (Illumina; >15 million reads per sample). As a control for background noise, input DNA (sheared chromatin that underwent all the crosslinking and sonication steps, but not immunoprecipitation) was included. Sequence alignment was performed as described above for the RNA-seq reads. The H3K27ac peaks of each sample were determined using MACS 2.0(Zhang et al., 2008) applying standard parameters, while controlling for experimental and technical bias. Differential peak analysis between unstimulated samples and cytokine-stimulated samples was performed using DiffBind in DESeq2 mode to detect differential peaks with an  $\text{FDR} \leq 0.01$ . H3K27ac profiles of representative genes were visualized using the integrative genomics viewer after normalization of bed files by total read count per sample(Robinson et al., 2011).

**Association between risk loci for autoimmune diseases and DEG clusters in IE-CTLs.** ImmunoChip summary statistics were downloaded from <https://www.immunobase.org/> and <https://www.ibdgenetics.org/> for several autoimmune disease traits: CeD, T1D, multiple sclerosis (MS), psoriasis (PSO), primary biliary cirrhosis (PBC), ankylosing spondylitis (AS), RA, IBD, ulcerative colitis (UC) and Crohn's Disease (CD)(Franke et al., 2010; Trynka et al., 2011; Tsoi et al., 2012; Eyre et al., 2012; Jostins et al., 2012; Liu et al., 2012, 2015; Beecham et al., 2013; Cortes et al., 2013; Goyette et al., 2015; Onengut-Gumuscu et al., 2015)44. For each trait, we pruned all genome-wide significant ( $5 \times 10^{-8}$ ) single nucleotide polymorphisms (SNPs) by chromosomal proximity (2 Mb) while selecting only the one with the lowest p-value per locus, which we defined as top-SNP. Next, we filtered out all SNPs from

non-autosomal chromosomes because not all of the genome-wide association studies (GWAS) had assessed the X chromosome. Then we defined all neighboring genes located within a window of 125 kilo bases (kb) on both sides of each top-SNP as GWAS-genes. Overlapping these GWAS-genes with the differentially expressed gene clusters from IE-CTL stimulation (as described in Figure 2), allowed us to calculate the number of top-SNPs for which GWAS-genes were present in each gene cluster. This frequency was converted to percentages by dividing by the total number of GWAS top-SNPs per autoimmune disease trait.

To ascertain the statistical significance of the percentage of GWAS top-SNPs represented in a given gene cluster, we computed an empirical null distribution of the expected percentage GWAS top-SNPs using randomized sets of genes. This empirical null distribution was calculated using 10,000 random gene sets, matching the exact same number of genomic regions as the query gene set (since genes are not randomly distributed throughout the genome). Finally, we calculated the percentage of GWAS top-SNPs represented in each of these random gene sets. Using this empirical null distribution, we were able to ascertain an empirical p-value by taking the number of times the null distribution had a higher percentage of overlaps with GWAS top-SNPs per autoimmune disease trait than the observed percentage with the queried gene clusters, divided by the total number of random gene sets ( $n=10,000$ ). This empirical p-value was then corrected for multiple testing using the FDR. By applying this method, we assessed the statistical significance of the overlapped percentage without bias for the number for genome wide loci in each trait and the number of genes per each transcriptional cluster.

## RESULTS

### **Tissue alarmins and adaptive cytokines induce distinct and shared responses in IE-CTLs**

To study the temporal transcriptional changes in CD8<sup>+</sup> IE-CTLs, we profiled IE-CTLs before and after stimulation with IFN $\beta$ , IL-15 or IL-21 at four time points (30 minutes, 3, 4 and 24 hrs). To ensure that optimal concentrations

of cytokines were used, we performed a titration experiment to select the minimum concentration of cytokines that induced maximal expression of a set of known marker genes (**Supplementary Fig. 1**). Using these optimal concentrations, we observed specific and distinct temporal transcriptional responses upon stimulation for all three stimuli (IFN $\beta$ , IL-15 and IL-21). Of note, no significant differences were observed in the transcriptome-wide PCA of CeD and healthy control samples for all time points (**Supplementary Fig. 2**), thus we combined all samples to perform differential gene expression analysis (**Fig. 1A and Supplementary Table.1**).

After 30 minutes of stimulation with IFN $\beta$  and IL-15, the expression of a relatively low number of genes was affected (27 and 50 DEGs, respectively;  $|\log_2 \text{Fold-change}| > 1$ ,  $\text{FDR} \leq 0.01$ ). In contrast, after 3 and 4 hrs of stimulation, both IFN $\beta$  and IL-15 promoted a strong transcriptional response (688 and 1,308 DEGs, respectively). However, the number of DEGs for IL-21 was very limited (only 144 genes after 3 hrs). Furthermore, while the IE-CTLs returned to a basal state after 24 hrs of IL-15 stimulation, IFN $\beta$  signaling was exacerbating after 24 hrs, with 2,018 DEGs (**Fig. 1A**). To visualize the overall dynamics of gene expression, we performed PCA using all the DEGs across all stimulations and time points (3,383 genes) (**Fig. 1B**). Consistent with the bar plots, the PCA revealed a modest but distinct change in gene expression upon IL-21 stimulation at all time points and strong but distinct responses upon IL-15 and IFN $\beta$  stimulation as indicated by the distance between the unstimulated and stimulated samples in PC1 and PC2. Each stimulation thus resulted in a unique gene expression profile, with the most dramatic effects induced by the tissue alarmins IL-15 and IFN $\beta$ .

Next, we evaluated the number of shared and unique genes modulated by each cytokine at each time point (**Fig. 1C and Supplementary Table 2**). We identified 128 common DEGs in response to the three different stimulations. Among these, we found genes implicated in the type 1 IFN response, including MX1, IFIT3 and STAT1; cytotoxicity genes like GZMB and NKTR; and genes contributing to proinflammatory pathways like TNF, TNFSF13B, LTB4R and the AP-1 transcription factor family members JUNB and BATF3 (**Supple-**

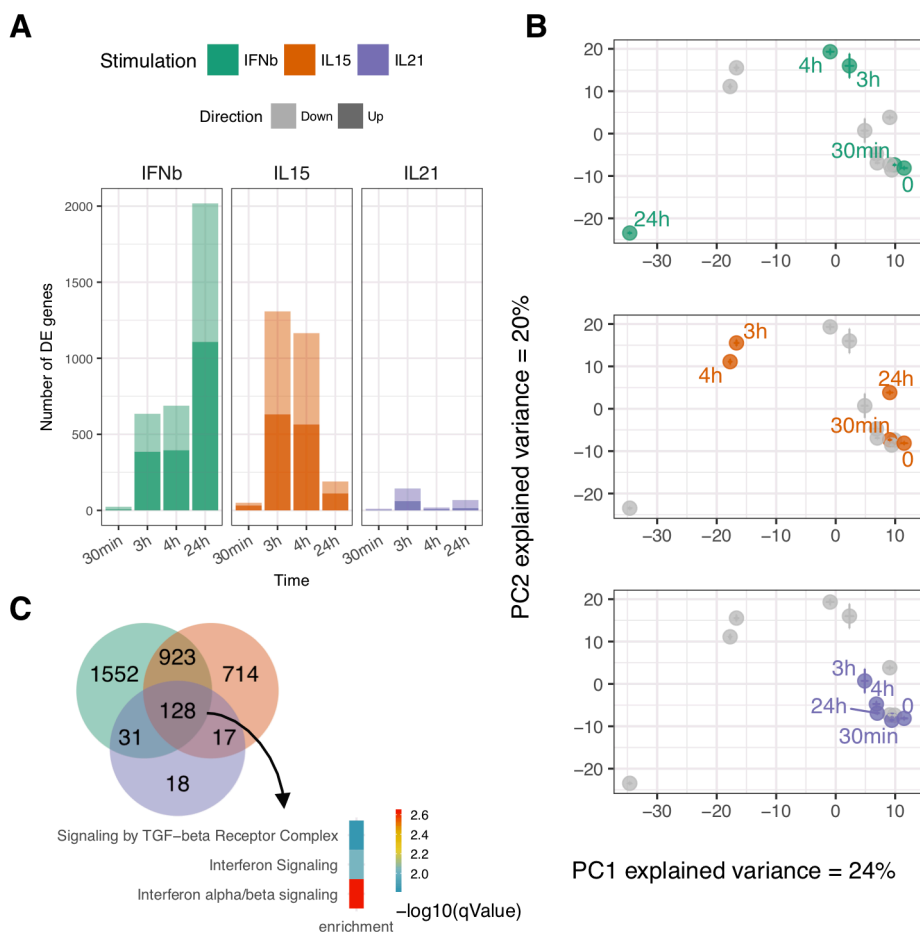


**Fig. 1 Distinct and common transcriptional response of IE-CTLs in response to tissue alarmins and adaptive cytokine.** After 12 days in culture, IE-CTLs were starved for 48 hrs then stimulated for 30 minutes, 3 hrs, 4 hrs or 24 hrs with IFN $\beta$ , IL-15 or IL-21. Unstimulated cells (0 hrs) were used as control. The transcriptome was analyzed by RNA-seq. (A) Number of DEGs after cytokine treatment in comparison with the unstimulated samples at each time point ( $|\log_2 \text{FC}| > 1$ ,  $\text{FDR} \leq 0.01$ ). Light colors indicate up-regulated genes. Dark colors indicate down-regulated genes. (B) Centroids of all the samples using Principal Components 1 and 2 from all DEGs reveal different time course patterns of gene expression upon IFN $\beta$  (green), IL-15 (orange) or IL-21 (purple) stimulation on IE-CTLs. (C) Venn diagram depicting the number of unique and overlapping genes across the stimulations and time points. The most significantly enriched pathways (determined by Reactome) of shared genes between the three stimulations are depicted. Color (key) indicates level of significance.

**mentary Table 2).** The largest overlap, with 923 shared DEGs, was observed between IL-15 and IFN $\beta$ , and these included additional antiviral response genes and cytokine and chemokine genes (e.g. MX2, OAS1, IFNG, IL18 and CCR5). Stimulus-specific DEGs were associated with various functions. For instance, some genes involved in T cell activation and coding for transcription factors were differentially induced by IL-15 (CD69, EGR1, LTA and LTB) and IFN $\beta$  (CD44, STAT2 and IL15). Furthermore, IL-21 specifically induced genes involved in general metabolic processes (SNRPA1 and CSDE1) and T cell activation (CD300A) (See supplementary Table 2 for a complete overview).

In summary, we demonstrate that cytokines up-regulated in the tissues targeted in organ-specific autoimmune disorders alter the expression of thousands of genes in IE-CTLs, even though these cells are terminally differentiated. Remarkably, tissue alarmins and IL-21 activate both shared and distinct transcriptional responses in IE-CTLs, with tissue alarmins having fundamentally a strong yet specific impact on the transcriptional program of IE-CTLs.

### **Alarmins and adaptive cytokines induce dynamic DEGs profiles in IE-CTLs**

To characterize dynamic gene expression changes in response to cytokines over time, for each stimulation we conducted unsupervised clustering analysis using the log2-fold changes observed between unstimulated samples and all time points. Furthermore, to understand the main biological processes induced upon stimulation with tissue alarmins and IL-21 in IE-CTLs, we performed gene set enrichment analysis (GSEA)(Subramanian et al., 2005) using Reactome Pathway analysis(Haw et al., 2011). Ten gene clusters were identified encompassing genes that followed distinct patterns (**Fig. 2A, B and Supplementary Table 3**). In general, we observed that time-dependent response patterns correspond to distinct biological pathways (**Fig. 2B and Supplementary Table 4**). Cluster 4 was marked by immediate early response gene (e.g. JUNB, IER2, FOS and EGR1)(Bahrami and Drabløs, 2016) activation at 30 min that was IL-15-specific, suggesting that these transcription



factors may regulate the IE-CTL response to IL-15 at 3 and 4 hrs. Clusters 1 (Butyrophilin family interactions), 5 (TGF- $\beta$  signaling) and 10 (protein synthesis and unfolded protein response) were primarily determined by genes responding to IL-15 as early as 3 hrs. In contrast, cluster 7 (antiviral pathways) and cluster 8 (cell cycle and proliferation) were genes primarily regulated by IFN $\beta$  at 3 and 24 hrs, respectively. Cluster 5 was the only cluster where we observed changes in gene expression in opposite directions, with genes being activated upon IL-15 stimulation and inhibited by IL-21 and IFN $\beta$  (**Fig. 2B and Supplementary Table 4**). Finally, cluster 9 (interferon and cytokine signaling) was characterized by DEGs responding to all three cytokines. No clusters specific to IL-21 stimulation were found (**Fig. 2A, B**), likely due to the minimal response of IE-CTLs to IL-21 stimulation (**Fig. 1A**). Of note, no pathway enrichment was found for clusters 2 and 3, which were consistently downregulated. However, some of the genes in these clusters are cytokine receptors and signal transducers (e.g. IL6ST, IL21R, UBASH3A and DGKZ), suggesting the existence of a negative feedback loop upon stimulation (**Fig. 2B**).

Together, this analysis identified 10 distinct clusters of gene expression patterns that are associated with specific biological pathways.

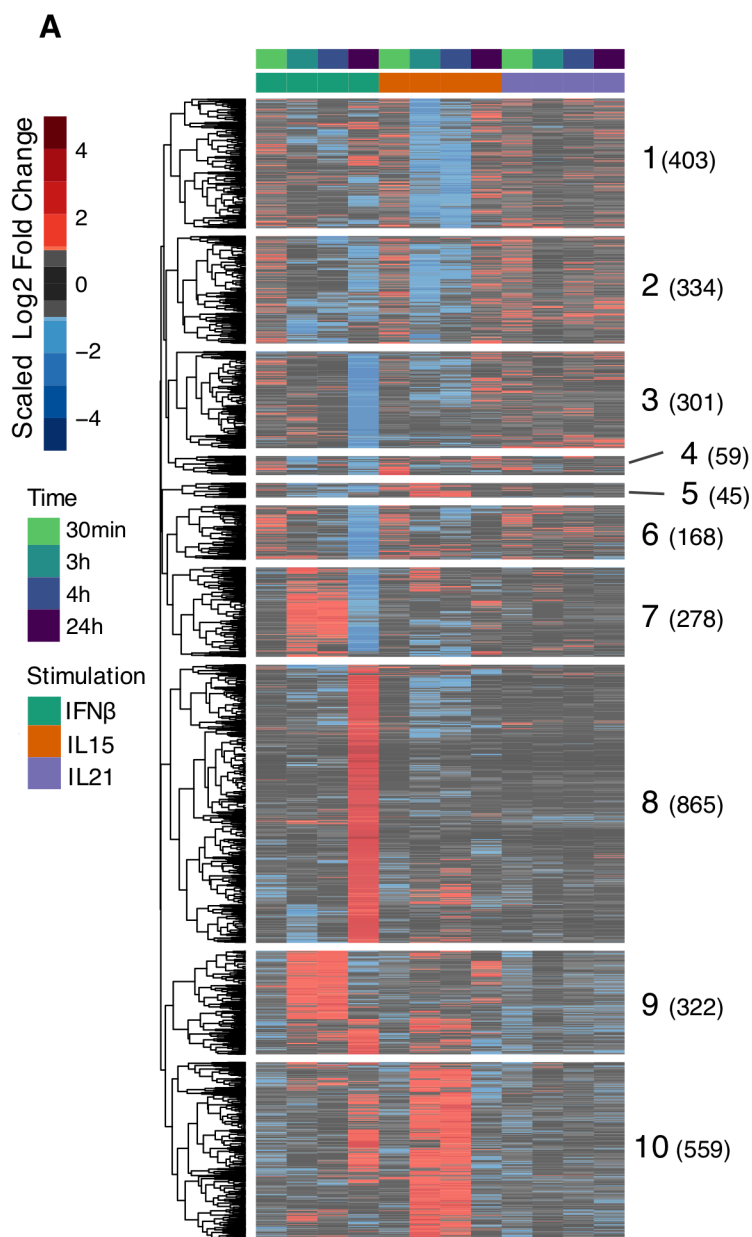
Alarmins and adaptive cytokine induce stimulus specific epigenetic profiles  
Having found that tissue alarmins, induce massive transcriptional changes in IE-CTLs, we sought to determine whether transcriptomic responses were associated with widespread changes in epigenetic profiles by performing H3K27ac ChIP-seq in unstimulated IE-CTLs and after 3 hrs of stimulation. H3K27ac is a mark associated with active promoters and enhancers, and is therefore indicative of the epigenetic activation state and regulation of gene expression (Core et al., 2014). We identified 20,840 H3K27ac peaks in unstimulated samples, while IFN $\beta$ , IL-15 or IL-21 treatment changed 2,147, 1,114, and 165 H3K27ac peaks significantly, respectively (FDR < 0.01, Fig. 3A and Supplementary Table 5), with 491, 208, and 60 of these being promoters and 908, 1657, and 106 of these defined as enhancers. Thus, gene expression changes were accompanied by significant changes in H3K27ac



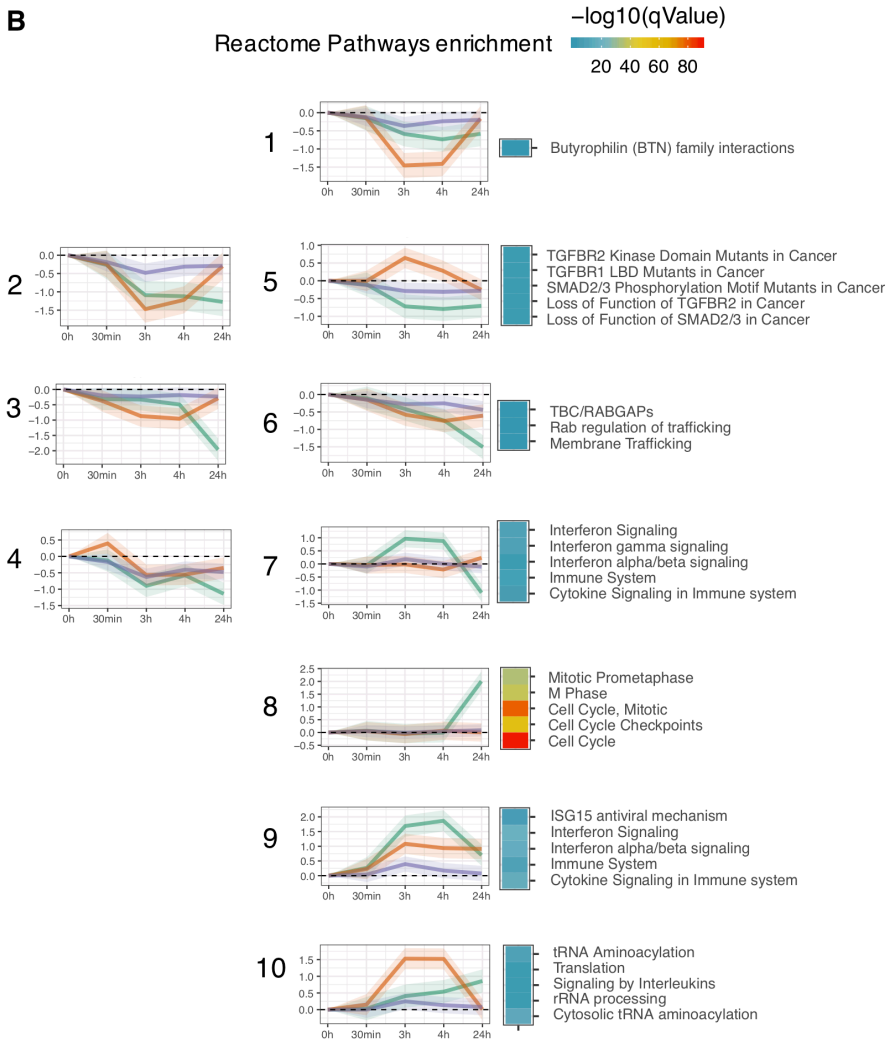
levels, but only in a subset of DEGs. Even though not all DEGs showed significant changes in H3K27ac levels, the PCA for peaks with differential levels of H3K27ac showed a clear distinction between stimulations, showing that these epigenetic profiles are indicative of the unique response of IE-CTLs to stimulations (**Fig. 3B**).

As the changes were most robust after stimulation with tissue alarmins, we focused our analysis in epigenetic changes upon IFN $\beta$  and IL-15 stimulation by linking H3K27ac promoter peaks with changes in gene expression (**Fig 3C**). Subsequently, we found that DEGs could be subdivided, based on significant changes in H3K27ac levels, into increased (Epi+), decreased (Epi-) and absence (EpiNA) of epigenetic changes (**Fig 3C-E and Supplementary Table 6**). **Strikingly**, the strongest and most robust upregulation in gene expression upon IFN $\beta$  stimulation was associated with increased levels of H3K27ac (**Fig. 3D**, top panels, and **Fig. 3E**). Conversely, for genes downregulated upon IFN $\beta$  and IL-15 stimulation, a decrease in gene expression was accompanied by a reduction in H3K27ac levels (**Supplementary Fig. 3A, B**). However, an increase in gene expression upon IL-15 stimulation was de-coupled from changes in levels of H3K27ac (p-values between gene expression levels of Epi+ and EpiNA genes were non-significant; **Fig. 3D**, bottom panels). This difference in behavior in H3K27ac levels of upregulated genes upon IFN $\beta$  and IL-15 stimulation could not be explained by epigenetic priming before stimulation (as assessed by H3K27ac levels at baseline; **Supplementary Fig. 3C**). Alternatively, gene expression could be regulated by non-coding RNAs (ncRNAs) (Almo et al., 2018; Hudson et al., 2019). Indeed, at 3 and 4 hrs of IL-15 stimulation, more ncRNAs were downregulated than upregulated, which suggests that ncRNAs stabilize gene expression of IL-15-inducible genes under unstimulated conditions. This was not observed after 3 and 4 hrs of IFN $\beta$  stimulation (**Supplementary Fig. 4**).

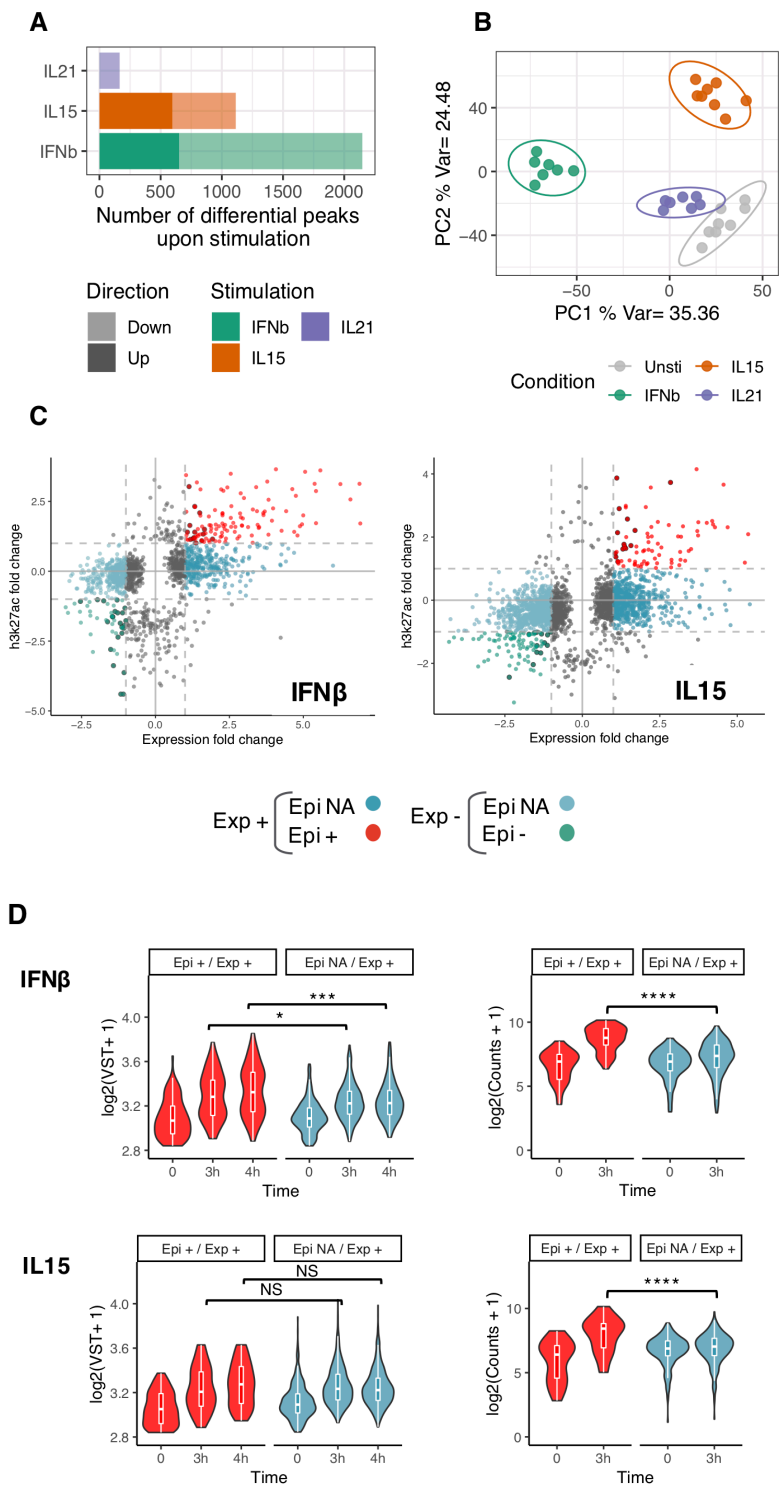
Taken together, our data suggest that gene expression effects are accompanied by significant changes in H3K27ac levels in promoters and enhancers for only a subset of DEGs and particularly upon IL-15 stimulation. This suggests that additional regulatory mechanisms need to be invoked.



(legend on next page)



**Fig. 2 Dynamic profile of DEGs in IE-CTLs in response to stimulation with tissue alarmins and adaptive cytokine.** (A) Unsupervised hierarchical clustering of all DEGs ( $|\log_2 \text{FC}| > 1$ ,  $\text{FDR} \leq 0.01$ ) across stimulations. Ten major clusters were defined as biologically relevant. Colors indicate scaled  $\log_2$  fold change in expression with respect to unstimulated samples, with red and blue indicative of a two-fold or more increase or decrease in expression, respectively. (B) Line plots illustrating the mean  $\log_2$  fold changes in expression of genes in a given cluster. Shades represent the standard error of the  $\log_2$  fold changes. Top 5 most significant pathways from GSA identified by Reactome ( $\text{q-value} \leq 0.01$ ) in DEGs (only clusters where enrichment was found are depicted). Colors (key) indicate significance.



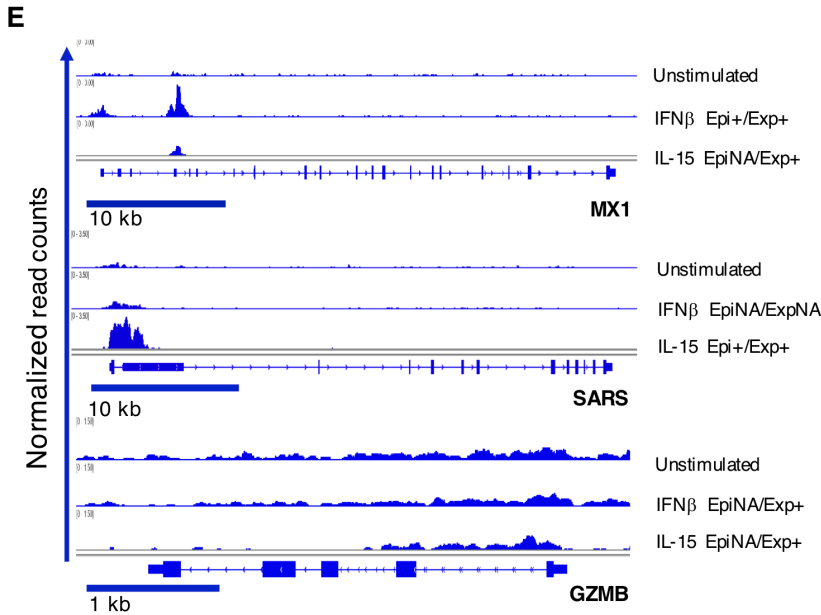


**Fig. 3 Specific epigenomic profiles induced by alarmins and adaptive cytokine.** All the differential H3K27ac peaks after 3 hrs of stimulation with IFN $\beta$ , IL-15 or IL-21 (FDR  $\leq$  0.01) are depicted in **(A)** barplots and **(B)** used for PCA to depict epigenetic responses of IE-CTLs upon stimulation. **(C)** Scatter plot displaying the association between changes in H3K27ac (Y-axis) and expression (X-axis) upon stimulation. Gene-peak pairs were grouped based on the direction of the fold change in expression (Exp+ and Exp-) and the direction (or lack of changes) in H3K27ac after stimulation (Epi+, Epi - and Epi NA). Red dots (Epi+ Exp+) indicate a fold change  $>1$  in both expression and H3K27ac occupancy. Green dots (Epi- Exp-) indicate a fold change  $<1$  in both expression and H3K27ac occupancy. Dark blue (Exp+ EpiNA) and light blue (Exp- EpiNA) are gene-peak pairs with fold change  $>1$  or  $<1$  in expression, respectively, and no change in H3K27ac. **(D)** Violin plots showing the distribution of gene expression levels (left, Log2(VST+1)) and H3K27ac occupation (right, Log2(Counts+1)) in up-regulated genes responding to IFN $\beta$  (upper panel) and IL-15 (lower panel) stimulation. Upregulated genes with H3K27 |fold change|  $>1$  (Epi+/Exp+) are shown in red and those without H3K27ac changes (EpiNA/Exp+) are shown in blue. Significant differences were assessed by Wilcoxon test (\*  $p < 0.05$ ; \*\*\*  $p < 0.01$ ; \*\*\*\*  $p < 0.001$ , NS non-significant). **(E)** Representative H3K27ac tracks illustrating the concordance between epigenomics and gene expression after IFN $\beta$  or IL-15 treatment.

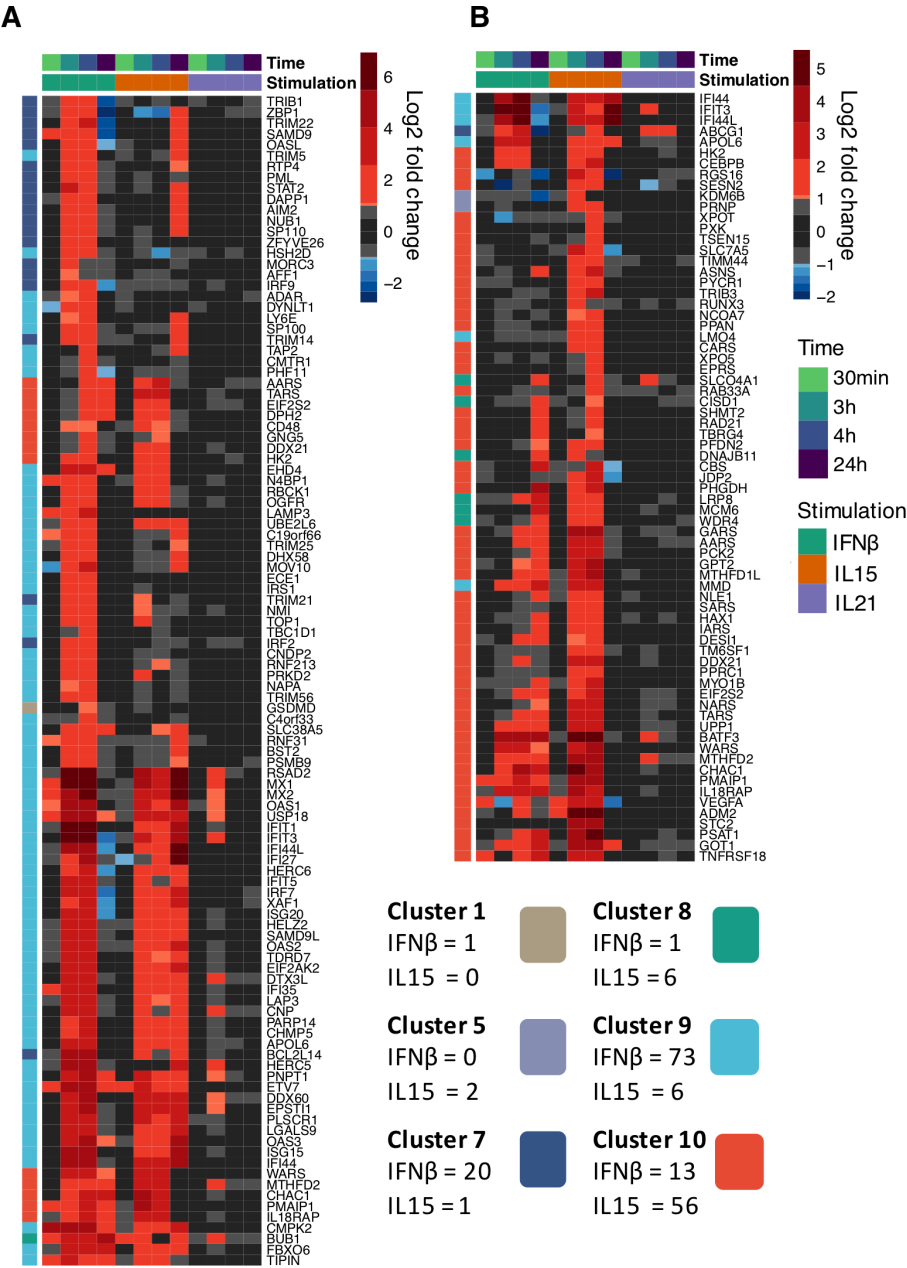
## **IL-15 and IFN $\beta$ induce specific transcriptional signatures though epigenetic changes in promoter regions**

We next wanted to see if the genes and pathways under strong epigenetic control were the same as those expressed upon stimulation with IFN $\beta$  and IL-15 (Epi+ genes in red, **Fig 3C**). Genes under epigenetic control upon stimulation with IFN $\beta$  or IL-15 were mostly unique per stimulus (with only 10 genes shared between IFN $\beta$  and IL-15), confirming that epigenetic changes are invoked differently between the two stimuli (**Fig 4A, B**). Strikingly, genes under epigenetic control were strongly enriched in certain DEG clusters, with epigenetically controlled genes upon IFN $\beta$  and IL-15 stimulation belonging predominantly to clusters 9 and 10, respectively (**Fig. 4A, B**). This was also reflected in the enriched pathways for genes under epigenetic control. IFN $\beta$  Epi+ genes were strongly enriched for antiviral, innate and interferon response pathways (**Fig. 4C**), whereas IL-15 Epi+ genes primarily play a role in pathways associated with protein synthesis (**Fig. 4D**).

Thus, distinct transcriptional and regulatory programs are initiated upon stimulation of IE-CTLs with tissue alarmins.

## **Autoimmune disease loci are enriched with DEGs of IE-CTLs stimulated with the alarmins IL-15 and IFN $\beta$ and adaptive cytokine IL-21**

SNPs associated with autoimmune diseases mark loci that contain genes that potentially contribute to the deregulated immune responses in disease-associated cell types. To calculate the enrichment of DEGs in autoimmune disease loci, we tested whether our 10 clusters of DEGs (**Fig. 2**) contained genes that also reside in loci associated with ten common autoimmune diseases (CeD, T1D, MS, IBD, UC, CD, PSO, PBC, AS and RA; all loci identified by ImmunoChip analysis) 34–44. We found significant overlap with one or more autoimmune diseases for all our DEG clusters except cluster 4 (**Supplementary Fig. 5A**). The large overlap between DEG clusters and autoimmune disease loci is not surprising as genetic loci associated with autoimmune diseases are often shared (Ricaño-Ponce and Wijmenga, 2013) and



(legend on next page)

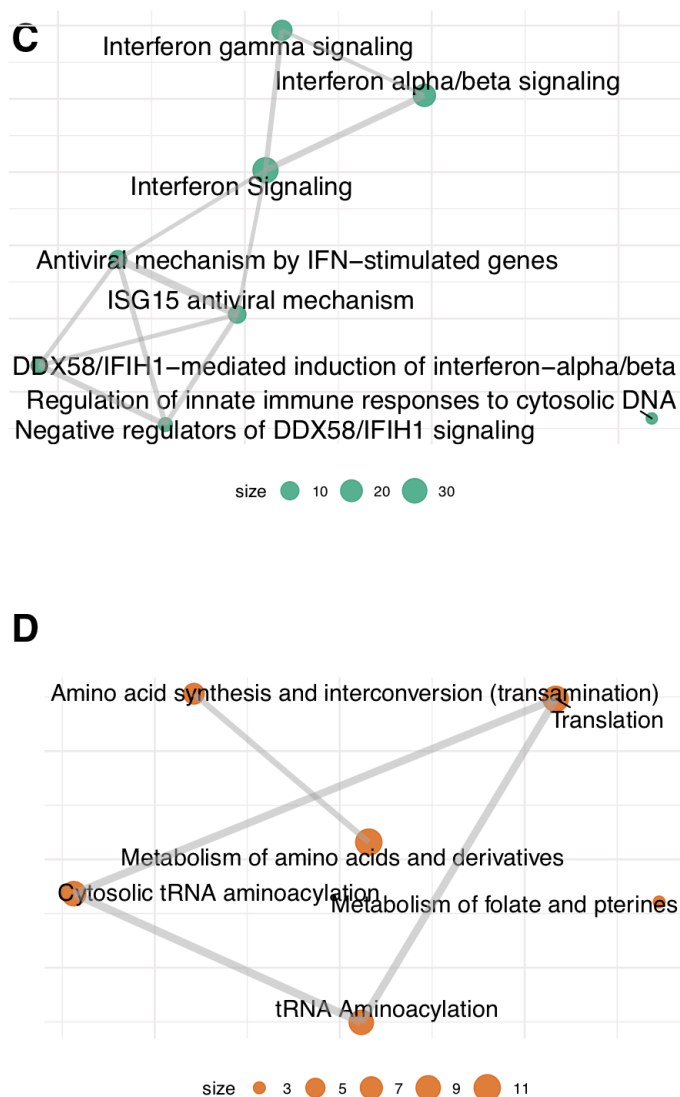


**Fig. 4 Alarmin-induced genes and biological pathways potentially regulated by epigenetic modifications.** Heatmap showing the differential expression at all time points of cytokine stimulation of **(A)** IFN $\beta$  and **(B)** IL-15 upregulated genes ( $\log_2$  FC >1, FDR  $\leq$  0.01) with concordant epigenomic changes (Epi+/Exp+). The number of Epi+/Exp+ genes per cluster are indicated. Network-based representation of enriched biological pathways identified by GSEA on Epi+/Exp+ genes responding to **(C)** IFN $\beta$  or **(D)** IL-15 stimulation.



enriched for immune-related genes. Moreover, CTLs have been implicated in multiple autoimmune diseases, including CeD, MS and T1D (Gianfrani et al., 2003; Salou et al., 2015; Pugliese, 2017). We noted that the genes participating in IFN-1 signaling (clusters 7 and 9) were enriched in loci associated with several autoimmune diseases, which is consistent with the pivotal role this pathway plays in the development and progression of immune mediated disorders (Hall and Rosen, no date).

Because the enrichment of DEGs in autoimmune risk loci can be driven by the same or by different genes per disease, we determined which individual genes overlap with autoimmune risk loci. Indeed, we found that cluster 2 DEGs were enriched in CeD, MS and PSO risk loci, but that these enrichments were caused by different genes (**Fig. 5**). Conversely, some immune regulators and cytokine/chemokine genes (e.g. REL, TNFRSF14, PTPN2 and CXCR5) were shared amongst multiple autoimmune disease loci, suggesting their involvement in common inflammatory processes that may trigger or maintain these diseases. Interestingly, we also found several non-immune related genes (e.g. TMEM181, ARHGAP9 and DNMT1) and ncRNAs (e.g. HOTAIRM1, RP11-335O4.3, RP13-516M14.1 and RP11-973H7.4) that were shared by many loci, implicating a role for these genes in autoimmune diseases. Other examples of DEGs in IE-CTLs that are associated with multiple autoimmune diseases are ICAM4 and RP11-973H7.4. Interestingly, genetic association of ICAM-4 levels in systemic lupus erythematosus (Kim et al., 2012) has been described previously, and RP11-973H7.4 has been implicated in the activation of T cells via modulation of the expression of MAP2K4 and the transcription factor ZEB1 (Houtman et al., 2018). Co-expression analysis also indicated a role for this ncRNA in T cell activation and cellular defense responses (**Supplementary Fig. 6A, B**).

In summary, our data has identified several potential gene targets that may play a unique and specific role in IE-CTLs and autoimmune disease etiology.

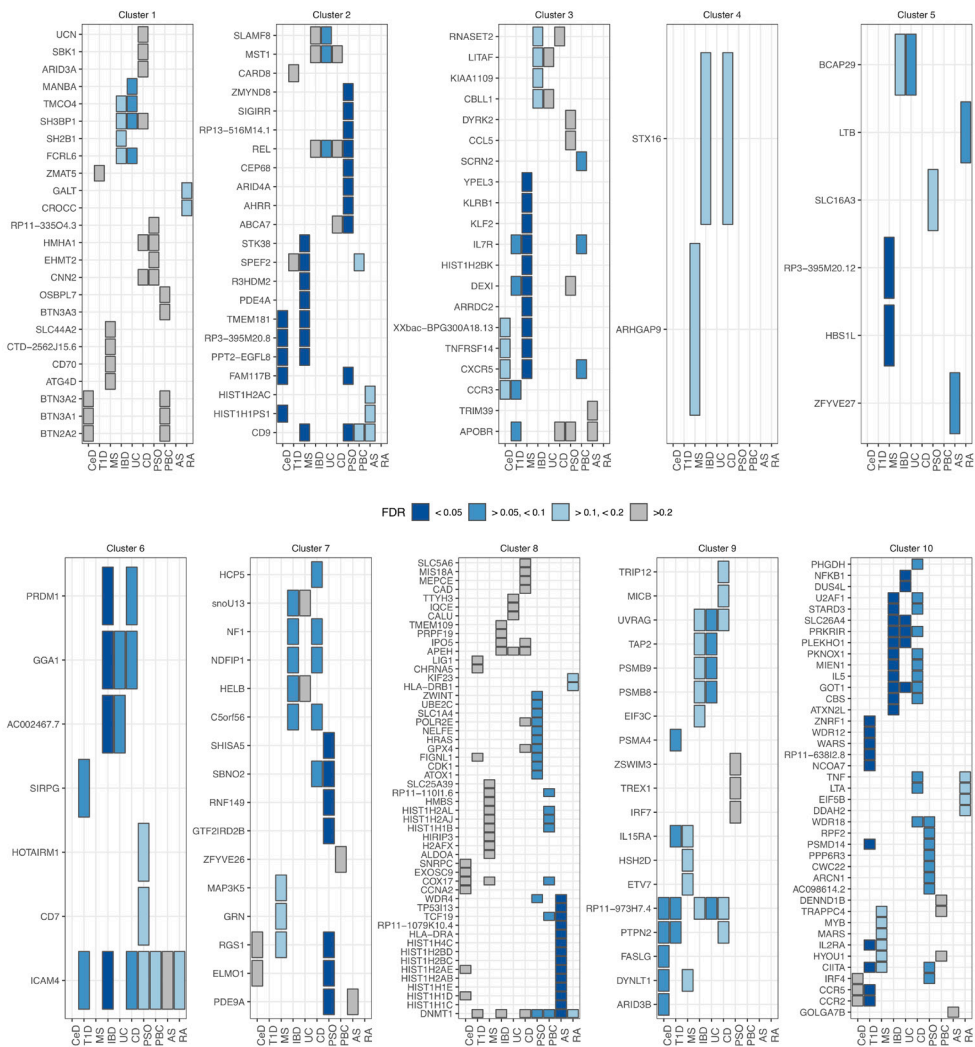


**Fig. 5 Risk loci for autoimmune diseases are enriched in clusters of DEGs responding to cytokine stimulation in IE-CTLs.** The overlap between autoimmune disease risk loci and the transcriptional response of IE-CTLs exposed to cytokines was calculated. Colors indicate the significance of the overlap between DEGs of clusters (**Fig. 2**) and genes in autoimmune risk loci. Diseases are shown on the X-axis and genes contributing to the overlap on the Y-axis.

enriched for immune-related genes. Moreover, CTLs have been implicated in multiple autoimmune diseases, including CeD, MS and T1D (Gianfrani et al., 2003; Salou et al., 2015; Pugliese, 2017). We noted that the genes participating in IFN-1 signaling (clusters 7 and 9) were enriched in loci associated with several autoimmune diseases, which is consistent with the pivotal role this pathway plays in the development and progression of immune mediated disorders (Hall and Rosen, no date).

Because the enrichment of DEGs in autoimmune risk loci can be driven by the same or by different genes per disease, we determined which individual genes overlap with autoimmune risk loci. Indeed, we found that cluster 2 DEGs were enriched in CeD, MS and PSO risk loci, but that these enrichments were caused by different genes (**Fig. 5**). Conversely, some immune regulators and cytokine/chemokine genes (e.g. REL, TNFRSF14, PTPN2 and CXCR5) were shared amongst multiple autoimmune disease loci, suggesting their involvement in common inflammatory processes that may trigger or maintain these diseases. Interestingly, we also found several non-immune related genes (e.g. TMEM181, ARHGAP9 and DNMT1) and ncRNAs (e.g. HOTAIRM1, RP11-335O4.3, RP13-516M14.1 and RP11-973H7.4) that were shared by many loci, implicating a role for these genes in autoimmune diseases. Other examples of DEGs in IE-CTLs that are associated with multiple autoimmune diseases are ICAM4 and RP11-973H7.4. Interestingly, genetic association of ICAM-4 levels in systemic lupus erythematosus (Kim et al., 2012) has been described previously, and RP11-973H7.4 has been implicated in the activation of T cells via modulation of the expression of MAP2K4 and the transcription factor ZEB1 (Houtman et al., 2018). Co-expression analysis also indicated a role for this ncRNA in T cell activation and cellular defense responses (**Supplementary Fig. 6A, B**).

In summary, our data has identified several potential gene targets that may play a unique and specific role in IE-CTLs and autoimmune disease etiology.

## DISCUSSION

This study aimed to compare dynamic transcriptional responses to two key tissue alarmins, IL-15 and IFN $\beta$ , and IL-21, a cytokine produced by CD4 $^{+}$  T cells, in human-tissue-resident IE-CTLs. This is particularly relevant in the context of organ-specific autoimmune disorders like CeD, where upregulation of the three cytokines is associated with tissue-resident CTL-mediated tissue destruction (Jabri and Abadie, no date; Jabri and Sollid, 2009). Two previous reports have studied the transcriptomic profile in freshly isolated IE-CTLs under resting conditions (Meresse et al., 2006; Raine et al., 2015). Furthermore, the transcriptional response to IL-15 and IL-21 had been analyzed in peripheral T cells in humans or mice, but not in tissue-resident CTLs. Finally, while a role for IFN $\beta$  in the activation of CTLs has been reported previously (Mescher et al., 2006), to our knowledge no genome-wide transcriptome analysis of IE-CTLs upon type-1 IFN stimulation had been performed. Overall, our analysis indicates that although tissue alarmins and adaptive cytokines both modulate the transcriptomic profile in IE-CTLs, the gene expression changes induced by the tissue alarmins IFN $\beta$  and IL-15 significantly exceed the changes caused by IL-21. Furthermore, IFN $\beta$ , IL-15 and IL-21 have the capacity to mediate distinct epigenetic and transcriptional changes in IE-CTLs, suggesting that they may play non-redundant, complementary roles in CTL-mediated tissue destruction. Finally, all three cytokines regulate a common core of genes involved in viral and interferon pathways that are enriched in autoimmune disease risk loci.

The observation that the tissue alarmins IFN $\beta$  and IL-15 have a more profound effect on IE-CTL than IL-21 suggests that tissue stress signals have a more direct impact on the regulation of IE-CTLs than cytokines produced by antigen-specific T cells. IL-15 regulates immediate-early response genes and temporarily induces metabolic, unfolded protein response (UPR) and amino-acid synthesis pathways. The UPR can trigger inflammatory signals and has been reported to occur in T cells activated by infection or excessive inflammation (Kamimura and Bevan, 2008; Grootjans et al., 2016). IFN $\beta$  induces a distinct transcriptional signature with an early type-1 interferon response,

followed by a more sustained upregulation of cell cycle genes at 24 hrs. The strong cell cycle and proliferative response to IFN $\beta$  after 24 hrs is in line with the massive expansion of CTLs observed in tissue destruction in autoimmune diseases (Gianfrani et al., 2003; Willcox et al., 2009; Salou et al., 2015; Pugliese, 2017). How the IFN $\beta$ -mediated type-1 interferon response impacts the function of IE-CTLs in tissue destruction remains to be determined. In contrast, IL-21 induced only 18 unique genes, which suggests that it mainly acts in cooperation with the tissue alarmins. The fact that IL-21 induces a limited reprogramming in CTLs (relative to IL-15 and IFN $\beta$ ) and its absence in potential CeD, where intestinal morphology is conserved (Sperandeo et al., 2011), suggest that IL-21 may not be involved at disease onset but in the development of tissue destruction via cooperation with tissue alarmins. Epigenetic changes in H3K27ac levels at enhancers and promoters were very modest after 3 hrs of stimulation with IFN $\beta$ , IL-15 and IL-21. Indeed, IL-15 induces the strongest transcriptional response after 3 and 4 hrs of stimulation, yet the majority of these DEGs did not display striking changes in the levels of H3K27ac. This contrasts sharply to naïve CD8 $^{+}$  T cells, where profound changes in epigenetic marks are readily observed upon stimulation (Cuddapah, Barski and Zhao, 2010), implying that mechanisms other than epigenetic changes are necessary to induce dynamic transcriptional programs in terminally differentiated effector IE-CTLs. Possible alternative regulatory mechanisms include regulation by ncRNAs. Indeed, a recent study identified ncRNAs uniquely expressed in different subsets of human CD8 $^{+}$  T cells upon activation (Hudson et al., 2019). Similarly, we found several differentially expressed ncRNA genes, including some located in genomic loci associated with autoimmune disease risk. Of note, we identified significant downregulated ncRNAs upon 3 and 4 hrs of IL-15 stimulation, which suggests that ncRNAs may have a specific role in IL-15-induced gene regulation that is independent of H3K27ac epigenetic modifications.

We further observed that all three cytokines promoted a common core of IFN immune response genes. Strikingly, these genes are also present in genomic risk loci associated with CeD, T1D, MS, IBD and UC. This suggests a critical role for IFN signaling in these autoimmune disorders and implies

that all three cytokines could cooperate to fully activate these pathways and endow CTLs with the ability promote tissue destruction. Moreover, ncRNAs were found to contribute to the enrichment of DEGs in autoimmune risk loci. Although the role of most ncRNAs is unknown, we inferred potential functions of these ncRNAs by performing co-expression network analysis with GeneNetwork (Deelen et al., 2018). For instance, the ncRNA RP11-973H7.4 was found to be involved in immune activation pathways that include TNF and MAPK signaling (Sabio and Davis, 2014). These findings further underscore the relevance of these transcripts in the regulation of gene expression and IE-CTL activation.

Overall, our approach elucidates the transcriptional responses of IE-CTLs to individual alarmins and cytokines, that are pivotal to the inflammation and tissue-destruction associated with autoimmune disease. We show that the alarmins IFN $\beta$  and IL-15 released from injured, infected or stressed epithelial cells may, in turn, trigger massive and numerous non-redundant changes in the transcriptional program of IE-CTLs. This suggests that they may play a critical role regulating IE-CTLs, and more generally tissue-resident CTLs, in organ-specific autoimmune disorders. Conversely, IL-21, a cytokine produced by CD4<sup>+</sup> T helper cells, may work collaboratively with alarmins on IE-CTLs. Our study emphasizes the need to investigate the mechanisms that underlie transcriptional changes in terminally differentiated tissue-resident CTLs, as our results suggest that these differ from those that govern the regulation of gene expression from naïve and memory CD8<sup>+</sup> T cells. Our approach teases apart specific responses and mechanisms regulated by these crucial alarmins and cytokines and provides unique insights into the interplay between IE-CTLs and cytokines present in the diseased tissue in organ-specific autoimmune disorders.

## **AUTHORS CONTRIBUTIONS**

M.M.Z., R.A.G, I.J, Y.L, S.W, B.J and C.W. envisioned this project and coordinated the research with input from all authors. T.M. and C.C. provided cell line expansions and assistance in the experiments. R.A.G. and Y.L. performed

the bioinformatics analysis and interpreted the data. M.M.Z. performed the cell line expansion and performed the stimulations, sample downstream processing, RNA-seq and ChIP-seq libraries. M.M.Z., R.A.G, C.W, B.J. and I.J. wrote the manuscript with input from all co-authors. All authors have read and agreed on the manuscript.

## ACKNOWLEDGMENTS

We thank Kate McIntyre for editorial assistance and Morris Swertz for data storage.

M.Z. is supported by an FP7/2007-2013/European Research Council (ERC) Advanced Grant (agreement 2012-322698). R.A.G is supported by CONA-CYT-I2T2 scholarship (382117). T.M. is supported by the US National Institutes of Health (T32 AI07090). S.W. is supported by the Netherlands Organization for Scientific Research (NWO) Gravity Grant 'NOCI' 670229 (file: 024.003.001). Y.L. is supported by a Radboud University Medical Centre Hypatia Tenure Track Grant [2018]. C.W. is supported a FP7/2007-2013/ERC Advanced Grant (agreement 2012-322698), the Stiftelsen K.G. Jebsen Coeliac Disease Research Centre (Oslo, Norway), an NWO Spinoza Prize (NWO SPI 92-266), the NWO Gravity Grant 'NOCI' 670229 (file: 024.003.001) and a UEG research prize (801449). B.J. Is supported by a Cancer Center support grant (P30CA014599), the Digestive Diseases Research Core Center at the University of Chicago (P30 DK42086) and the US National Institutes of Health (RO1 DK67180 and R01 DK098435). I.J. is supported by a Rosalind Franklin Fellowship from the University of Groningen and an NWO VIDI grant (016.171.047).

## COMPETING INTERESTS

B. J. is an advisor to Immusan T, BIONIZ therapeutics and Actobio therapeutics.

## REFERENCES

Almo, M. M. et al. (2018) 'The role of long noncoding RNAs in human T CD3+

cells', *Journal of Immunological Sciences*, 2(1), pp. 32–36. doi: 10.29245/2578-3009/2018/2.1.1109.

Anders, S. and Huber, W. (2010) 'Differential expression analysis for sequence count data', *Genome Biology*, 11(10). doi: 10.1186/gb-2010-11-10-r106.

Anders, S., Pyl, P. T. and Huber, W. (2015) 'HTSeq-A Python framework to work with high-throughput sequencing data', *Bioinformatics*, 31(2), pp. 166–169. doi: 10.1093/bioinformatics/btu638.

Bahrami, S. and Drabløs, F. (2016) 'Gene regulation in the immediate-early response process', *Advances in Biological Regulation*. Pergamon, 62, pp. 37–49. doi: 10.1016/J.JBIOR.2016.05.001.

Beecham, A. H. et al. (2013) 'Analysis of immune-related loci identifies 48 new susceptibility variants for multiple sclerosis', *Nature Genetics*, 45(11), pp. 1353–1360. doi: 10.1038/ng.2770.

Berard, M. et al. (2003) 'IL-15 Promotes the Survival of Naive and Memory Phenotype CD8+ T Cells', *The Journal of Immunology*, 170(10), pp. 5018–5026. doi: 10.4049/jimmunol.170.10.5018.

Bodd, M. et al. (2010) 'HLA-DQ2-restricted gluten-reactive T cells produce IL-21 but not IL-17 or IL-22', *Mucosal Immunology*, 3. doi: 10.1038/mi.2010.36.

Borrelli, M. et al. (2016) 'In the Intestinal Mucosa of Children With Potential Celiac Disease IL-21 and IL-17A are Less Expressed than in the Active Disease.', *The American journal of gastroenterology*, 111(1), pp. 134–44. doi: 10.1038/ajg.2015.390.

Ciechomska, M. and Skalska, U. (2018) 'Targeting interferons as a strategy for systemic sclerosis treatment', *Immunology Letters*, 195, pp. 45–54. doi: 10.1016/j.imlet.2017.10.011.

Core, L. J. et al. (2014) 'Analysis of nascent RNA identifies a unified architecture of initiation regions at mammalian promoters and enhancers', *Nature Genetics*. doi: 10.1038/ng.3142.

Cortes, A. et al. (2013) 'Identification of multiple risk variants for ankylosing spondylitis through high-density genotyping of immune-related loci', *Nature Genetics*, 45(7), pp. 730–738. doi: 10.1038/ng.2667.

Cuddapah, S., Barski, A. and Zhao, K. (2010) 'Epigenomics of T cell activation, differentiation, and memory', *Current Opinion in Immunology*, pp. 341–347. doi: 10.1016/j.coi.2010.02.007.



Deelen, P. et al. (2018) 'Improving the diagnostic yield of exome-sequencing, by predicting gene-phenotype associations using large-scale gene expression analysis', *bioRxiv*. doi: 10.1101/375766.

Eyre, S. et al. (2012) 'High-density genetic mapping identifies new susceptibility loci for rheumatoid arthritis', *Nature Genetics*, 44(12), pp. 1336–1340. doi: 10.1038/ng.2462.

Fan, X. and Rudensky, A. Y. (2016) 'Hallmarks of Tissue-Resident Lymphocytes.', *Cell*. NIH Public Access, 164(6), pp. 1198–1211. doi: 10.1016/j.cell.2016.02.048.

Franke, A. et al. (2010) 'Genome-wide meta-analysis increases to 71 the number of confirmed Crohn's disease susceptibility loci.', *Nature genetics*, 42(12), pp. 1118–25. doi: 10.1038/ng.717.

Gianfrani, C. et al. (2003) 'Celiac disease association with CD8+ T cell responses: identification of a novel gliadin-derived HLA-A2-restricted epitope.', *Journal of immunology (Baltimore, Md. : 1950)*, 170(5), pp. 2719–26. Available at: <http://www.ncbi.nlm.nih.gov/pubmed/12594302> (Accessed: 9 December 2018).

Goyette, P. et al. (2015) 'High-density mapping of the MHC identifies a shared role for HLA-DRB1\*01:03 in inflammatory bowel diseases and heterozygous advantage in ulcerative colitis.', *Nature genetics*, 47(2), pp. 172–9. doi: 10.1038/ng.3176.

Grootjans, J. et al. (2016) 'The unfolded protein response in immunity and inflammation.', *Nature reviews. Immunology*. NIH Public Access, 16(8), pp. 469–84. doi: 10.1038/nri.2016.62.

Hall, J. C. and Rosen, A. (no date) 'Type I interferons: crucial participants in disease amplification in autoimmunity'. doi: 10.1038/nrrheum.2009.237.

Haw, R. et al. (2011) 'Reactome pathway analysis to enrich biological discovery in proteomics data sets.', *Proteomics*. NIH Public Access, 11(18), pp. 3598–613. doi: 10.1002/pmic.201100066.

Houtman, M. et al. (2018) 'T cells are influenced by a long non-coding RNA in the autoimmune associated PTPN2 locus', *Journal of Autoimmunity*. Academic Press, 90, pp. 28–38. doi: 10.1016/j.jaut.2018.01.003.

Hoytema van Konijnenburg, D. P. and Mucida, D. (2017) Intraepithelial lymphocytes, *Current Biology*. doi: 10.1016/j.cub.2017.05.073.

Hudson, W. H. et al. (2019) 'Expression of novel long noncoding RNAs defines virus-specific effector and memory CD8<sup>+</sup> T cells', *Nature Communications*, 10(1). doi: 10.1038/s41467-018-07956-7.

Jabri, B. et al. (2000) 'Selective expansion of intraepithelial lymphocytes expressing the HLA-E-specific natural killer receptor CD94 in celiac disease', *Gastroenterology*, 118(5), pp. 867–879. doi: 10.1016/S0016-5085(00)70173-9.

Jabri, B. and Abadie, V. (no date) 'IL-15 functions as a danger signal to regulate tissue-resident T cells and tissue destruction', *Nat Rev Immunol*. doi: 10.1038/nri3919.

Jabri, B. and Meresse, B. (2006) 'NKG2 receptor-mediated regulation of effector CTL functions in the human tissue microenvironment.', *Current topics in microbiology and immunology*, 298, pp. 139–56. Available at: <http://www.ncbi.nlm.nih.gov/pubmed/16323414> (Accessed: 7 November 2018).

Jabri, B. and Sollid, L. M. (2009) 'Tissue-mediated control of immunopathology in coeliac disease', *Nature Reviews Immunology*. doi: 10.1038/nri2670.

Jostins, L. et al. (2012) 'Host-microbe interactions have shaped the genetic architecture of inflammatory bowel disease.', *Nature*, 491(7422), pp. 119–24. doi: 10.1038/nature11582.

Kamimura, D. and Bevan, M. J. (2008) 'Endoplasmic reticulum stress regulator XBP-1 contributes to effector CD8<sup>+</sup> T cell differentiation during acute infection.', *Journal of immunology* (Baltimore, Md. : 1950). NIH Public Access, 181(8), pp. 5433–41. Available at: <http://www.ncbi.nlm.nih.gov/pubmed/18832700> (Accessed: 8 October 2018).

Kim, D., Langmead, B. and Salzberg, S. L. (2015) 'HISAT: a fast spliced aligner with low memory requirements', *Nature Methods*, 12(4), pp. 357–360. doi: 10.1038/nmeth.3317.

Kim, K. et al. (2012) 'Variation in the ICAM1-ICAM4-ICAM5 locus is associated with systemic lupus erythematosus susceptibility in multiple ancestries.', *Annals of the rheumatic diseases*. NIH Public Access, 71(11), pp. 1809–14. doi: 10.1136/annrheumdis-2011-201110.

Li, H. et al. (2009) 'The Sequence Alignment/Map format and SAMtools', *Bioinformatics*, 25(16), pp. 2078–2079. doi: 10.1093/bioinformatics/btp352.

Liu, J. Z. et al. (2012) 'Dense fine-mapping study identifies new susceptibili-

ty loci for primary biliary cirrhosis', *Nature Genetics*, 44(10), pp. 1137–1141. doi: 10.1038/ng.2395.

Liu, J. Z. et al. (2015) 'Association analyses identify 38 susceptibility loci for inflammatory bowel disease and highlight shared genetic risk across populations', *Nature Genetics*, 47(9), pp. 979–986. doi: 10.1038/ng.3359.

Mayassi, T. and Jabri, B. (2018) 'Human intraepithelial lymphocytes', *Mucosal Immunology*. doi: 10.1038/s41385-018-0016-5.

Mention, J. J. et al. (2003) 'Interleukin 15: A key to disrupted intraepithelial lymphocyte homeostasis and lymphomagenesis in celiac disease', *Gastroenterology*. doi: 10.1016/S0016-5085(03)01047-3.

Meresse, B. et al. (2006) 'Reprogramming of CTLs into natural killer-like cells in celiac disease.', *The Journal of experimental medicine*, 203(5), pp. 1343–55. doi: 10.1084/jem.20060028.

Mescher, M. F. et al. (2006) 'Signals required for programming effector and memory development by CD8+ T cells', *Immunological Reviews*, pp. 81–92. doi: 10.1111/j.0105-2896.2006.00382.x.

Moudgil, K. D. and Choubey, D. (2011) 'Cytokines in Autoimmunity: Role in Induction, Regulation, and Treatment', *Journal of Interferon & Cytokine Research*, 31(10), pp. 695–703. doi: 10.1089/jir.2011.0065.

Onengut-Gumuscu, S. et al. (2015) 'Fine mapping of type 1 diabetes susceptibility loci and evidence for colocalization of causal variants with lymphoid gene enhancers', *Nature Genetics*, 47(4), pp. 381–386. doi: 10.1038/ng.3245.

Pouw, N. et al. (2010) 'Combination of IL-21 and IL-15 enhances tumour-specific cytotoxicity and cytokine production of TCR-transduced primary T cells', *Cancer Immunology, Immunotherapy*, 59(6), pp. 921–931. doi: 10.1007/s00262-010-0818-0.

Pugliese, A. (2017) 'Autoreactive T cells in type 1 diabetes', *The Journal of Clinical Investigation*. American Society for Clinical Investigation, 127(8), pp. 2881–2891. doi: 10.1172/JCI94549.

Raine, T. et al. (2015) 'Generation of primary human intestinal T cell transcriptomes reveals differential expression at genetic risk loci for immune-mediated disease', *Gut*, 64, pp. 250–259. doi: 10.1136/gutjnl-2013-306657.

Ricaño-Ponce, I. and Wijmenga, C. (2013) 'Mapping of immune-mediated disease genes.', *Annual review of genomics and human genetics*, 14(1), pp.

325–53. doi: 10.1146/annurev-genom-091212-153450.

Roberts, A. I. et al. (2001) 'Cutting Edge: NKG2D Receptors Induced by IL-15 Costimulate CD28-Negative Effector CTL in the Tissue Microenvironment', *The Journal of Immunology*. doi: 10.4049/jimmunol.167.10.5527.

Robinson, J. T. et al. (2011) 'Integrative genomics viewer', *Nature Biotechnology*, 29(1), pp. 24–26. doi: 10.1038/nbt.1754.

Di Sabatino, A. et al. (2006) 'Epithelium derived interleukin 15 regulates intraepithelial lymphocyte Th1 cytokine production, cytotoxicity, and survival in coeliac disease', *Gut*, 55, pp. 469–477. doi: 10.1136/gut.2005.068684.

Di Sabatino, A. et al. (2007) 'Evidence for the Role of Interferon-alfa Production by Dendritic Cells in the Th1 Response in Celiac Disease', *Gastroenterology*, 133(4), pp. 1175–1187. doi: 10.1053/j.gastro.2007.08.018.

Sabio, G. and Davis, R. J. (2014) 'TNF and MAP kinase signalling pathways.', *Seminars in immunology*. NIH Public Access, 26(3), pp. 237–45. doi: 10.1016/j.smim.2014.02.009.

Salou, M. et al. (2015) 'Involvement of CD8(+) T Cells in Multiple Sclerosis.', *Frontiers in immunology*. Frontiers Media SA, 6, p. 604. doi: 10.3389/fimmu.2015.00604.

Setty, M. et al. (2015) 'Distinct and Synergistic Contributions of Epithelial Stress and Adaptive Immunity to Functions of Intraepithelial Killer Cells and Active Celiac Disease.', *Gastroenterology*, 149(3), p. 681–91.e10. doi: 10.1053/j.gastro.2015.05.013.

Sheridan, B. S. and Lefrançois, L. (2010) 'Intraepithelial lymphocytes: to serve and protect.', *Current gastroenterology reports*. NIH Public Access, 12(6), pp. 513–21. doi: 10.1007/s11894-010-0148-6.

Sperandeo, M. P. et al. (2011) 'Potential Celiac Patients: A Model of Celiac Disease Pathogenesis', *PLoS ONE*. Edited by C. Schönbach, 6(7), p. e21281. doi: 10.1371/journal.pone.0021281.

Subramanian, A. et al. (2005) 'Gene set enrichment analysis: A knowledge-based approach for interpreting genome-wide expression profiles', *Proceedings of the National Academy of Sciences*, 102(43), pp. 15545–15550. doi: 10.1073/pnas.0506580102.

Trynka, G. et al. (2011) 'Dense genotyping identifies and localizes multiple common and rare variant association signals in celiac disease', *Nature Ge-*

netics, 43(12), pp. 1193–1201. doi: 10.1038/ng.998.

Tsai, S., Shameli, A. and Santamaria, P. (2008) 'CD8+ T Cells in Type 1 Diabetes', in *Advances in immunology*, pp. 79–124. doi: 10.1016/S0065-2776(08)00804-3.

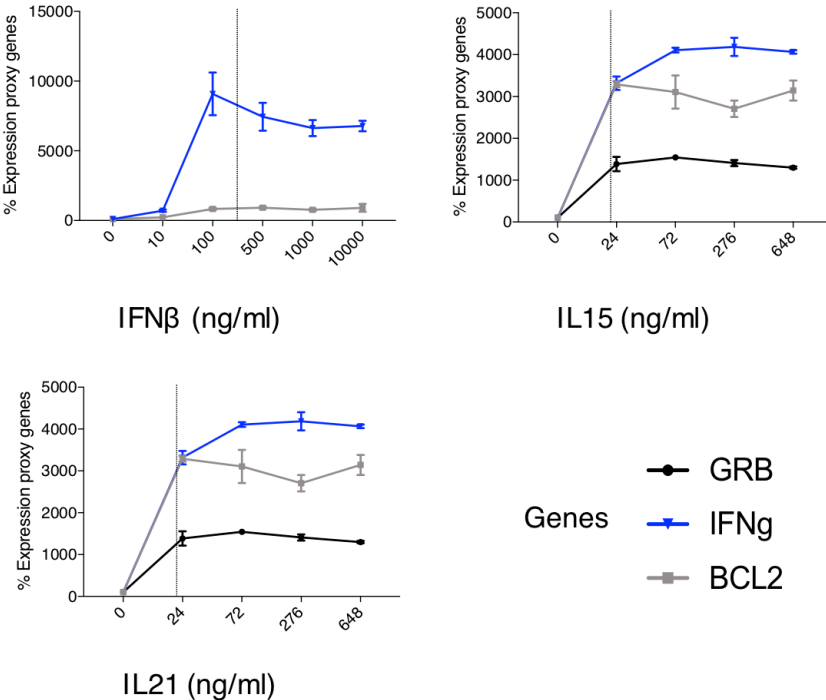
Tsoi, L. C. et al. (2012) 'Identification of 15 new psoriasis susceptibility loci highlights the role of innate immunity', *Nature Genetics*, 44(12), pp. 1341–1348. doi: 10.1038/ng.2467.

Willcox, A. et al. (2009) 'Analysis of islet inflammation in human type 1 diabetes.', *Clinical and experimental immunology*. Wiley-Blackwell, 155(2), pp. 173–81. doi: 10.1111/j.1365-2249.2008.03860.x.

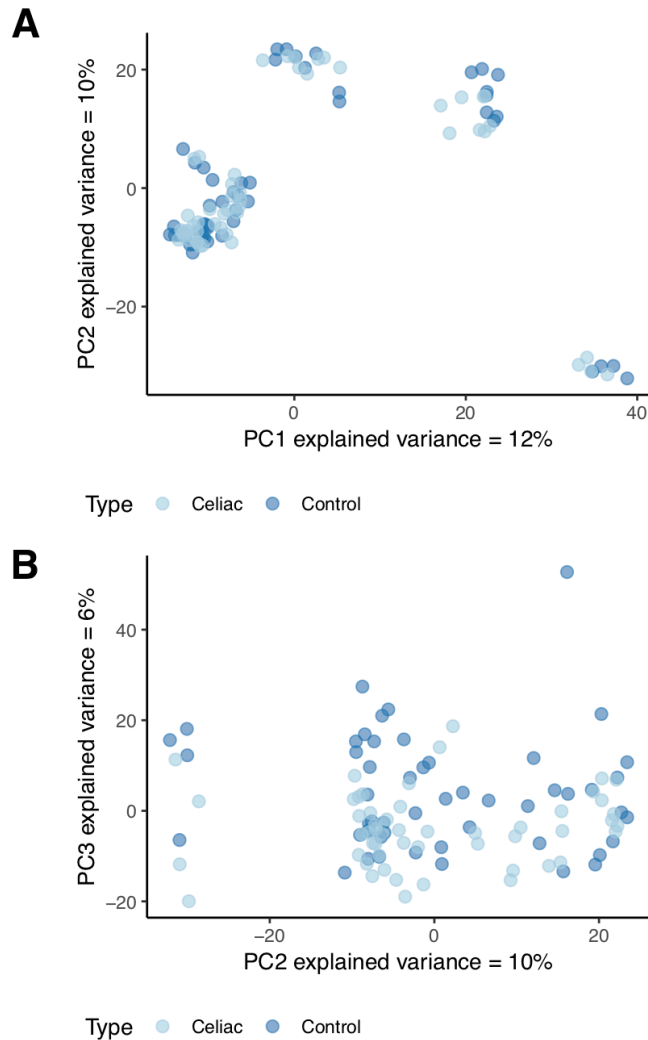
Yuan, F.-L. et al. (2011) 'Targeting interleukin-21 in rheumatoid arthritis', *Molecular Biology Reports*, 38(3), pp. 1717–1721. doi: 10.1007/s11033-010-0285-x.

Zhang, Y. et al. (2008) 'Model-based analysis of ChIP-Seq (MACS)', *Genome Biology*, 9(9). doi: 10.1186/gb-2008-9-9-r137.

## Supplemental Figures



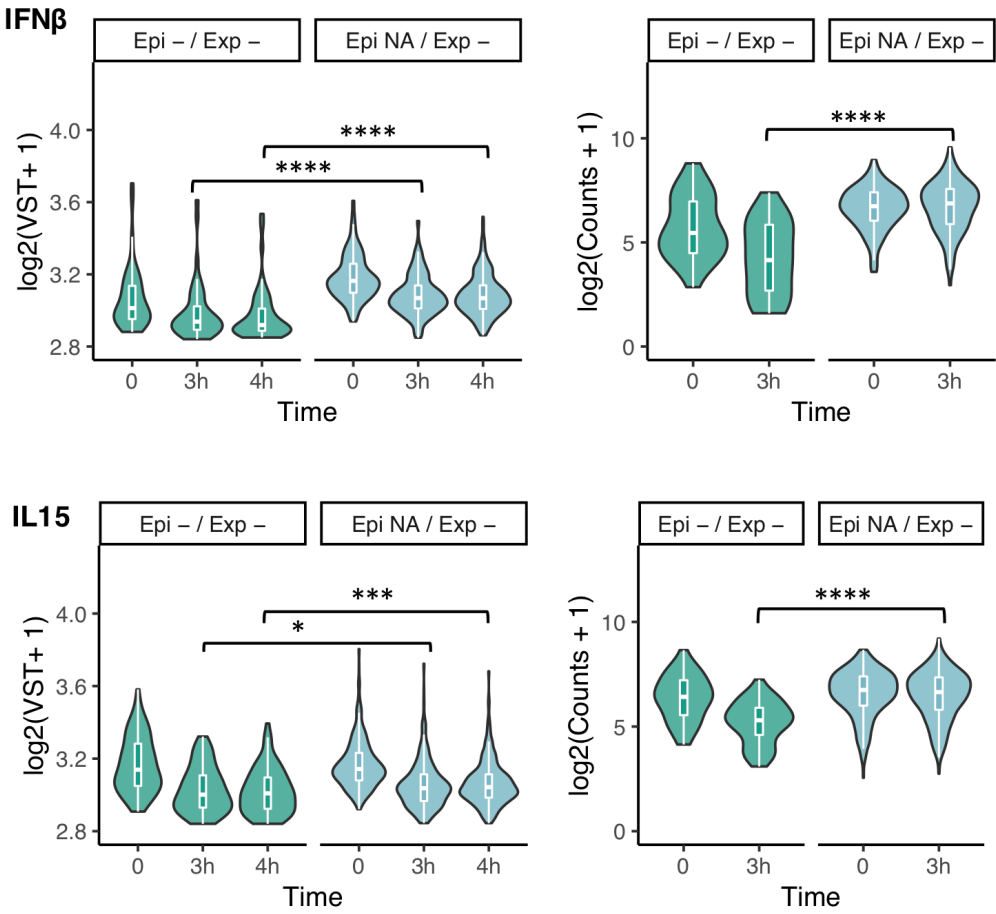
**Supplementary Fig. 1 Cytokine titration.** Following 12 days in culture, the IE-CTLs were starved for 48 hrs, then stimulated for 3 hrs with different concentrations of IFN $\beta$ , IL-15, or IL-21 (ng/ml). The gene expression of marker genes was evaluated by qPCR (IFN $\gamma$ , GRB, BCL2). The expression of each gene was normalized against GAPDH. The  $\Delta\Delta$  CT values are shown as percentages in the Y-axis, using the unstimulated cells as reference (100% expression). Error bars indicate the standard deviation of technical triplicates. The concentrations of cytokines used for the RNA-seq and ChIP-seq experiments are indicated with a dotted line.



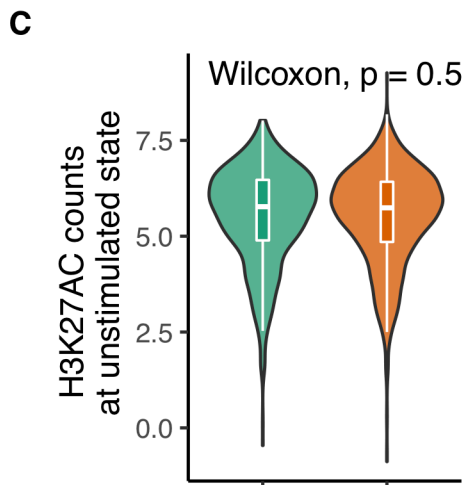
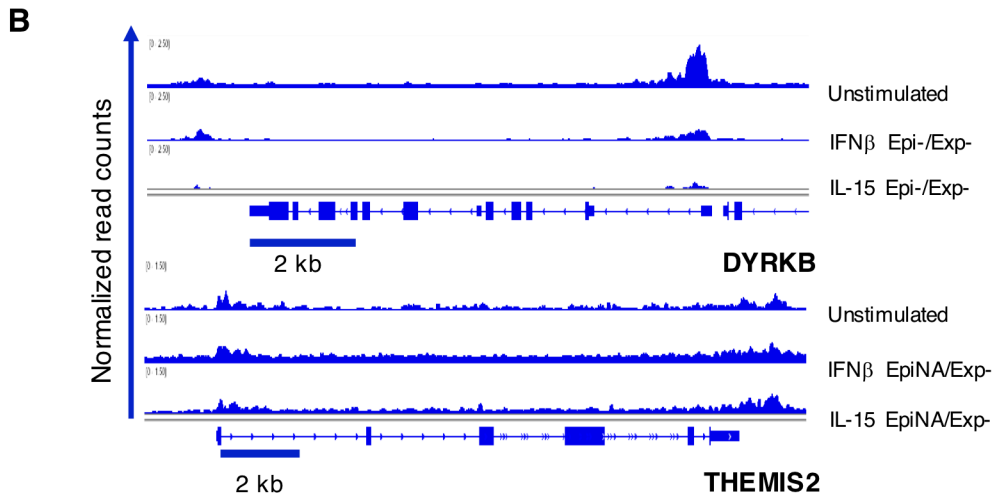
**Supplementary Fig. 2 Transcriptional profile in CeD patients and healthy controls.** PCA showing the overall genome-wide transcriptome of all IE-CTL samples derived from CeD patients and healthy controls across the different time points and cytokine treatments.



**A**

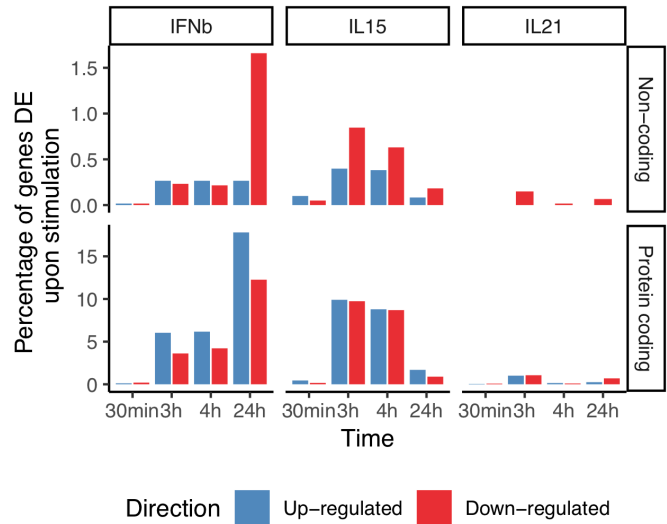


(legend on next page)



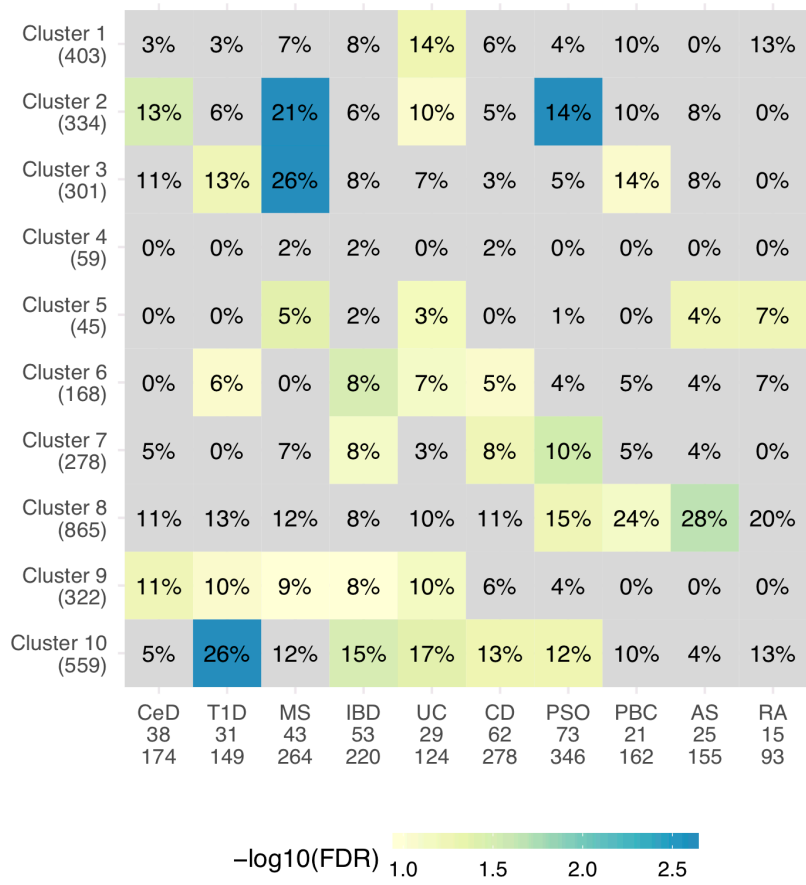
**Supplementary Fig. 3 H3K27ac in down-regulated genes upon cytokine stimulation.**

**(A)** Distribution of gene expression levels (left,  $\text{Log}_2(\text{VST}+1)$ ) and H3K27ac levels (right  $\text{Log}_2(\text{Counts}+1)$ ) in down-regulated genes responding to IFN $\beta$  (upper panel) and IL-15 (lower panel). Downregulated genes with  $|\text{fold change}| < 1$  (Epi-/Exp-) are shown in green and those with no change (EpiNA/Exp-) in H3K27ac are shown in blue. Significant differences were assessed by Wilcoxon test (\*  $p < 0.05$ ; \*\*\*  $p < 0.01$ ; \*\*\*\*  $p < 0.001$ ). **(B)** Representative H3K27ac tracks illustrating the concordance between epigenomics and gene expression after IFN $\beta$  or IL-15 treatment. **(C)** Distribution of H3K27ac levels in promoter peak of DEGs upon 3 and 4 hrs stimulation with IFN $\beta$  (green) or IL-15 (orange) at baseline conditions. P-value calculated by Wilcoxon test.



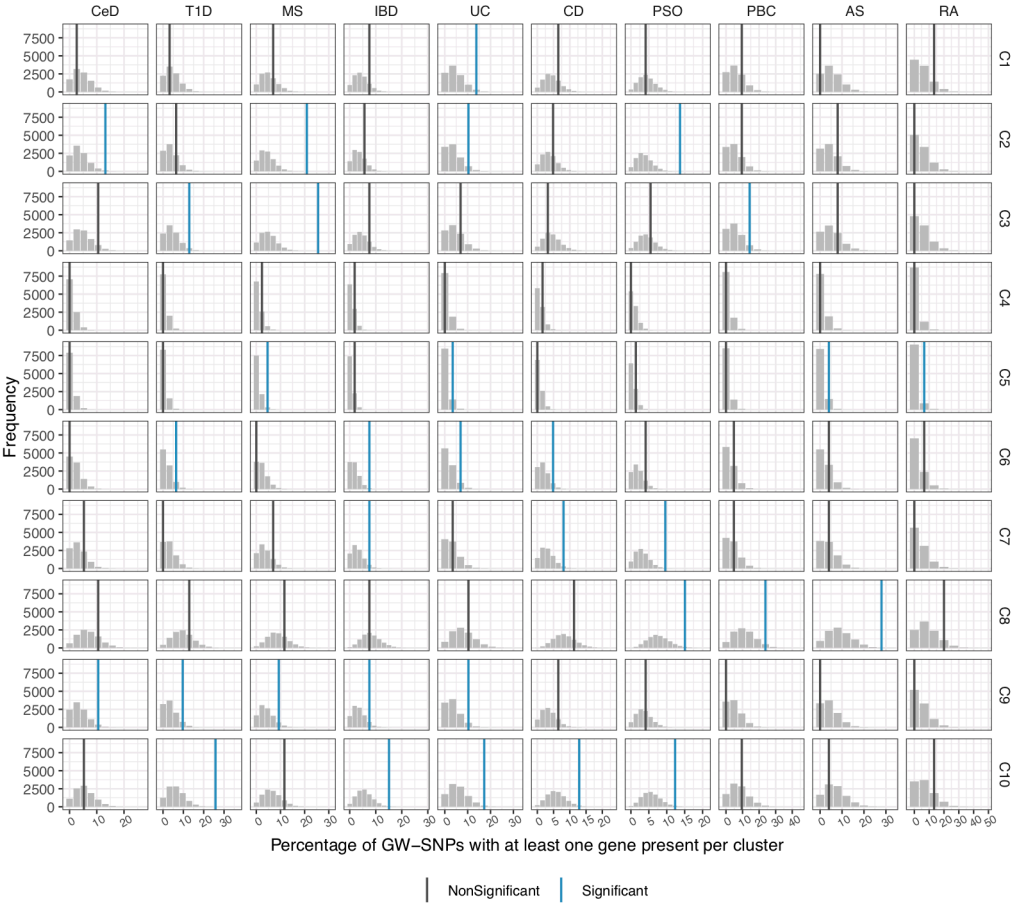
**Supplementary Fig. 4 Non-coding and protein coding genes responding to cytokine stimulation.** Bar-plots showing the percentage of protein coding and non-coding genes among all DEGs per cytokine stimulation. Red and blue indicate up-regulated or down-regulated genes, respectively.

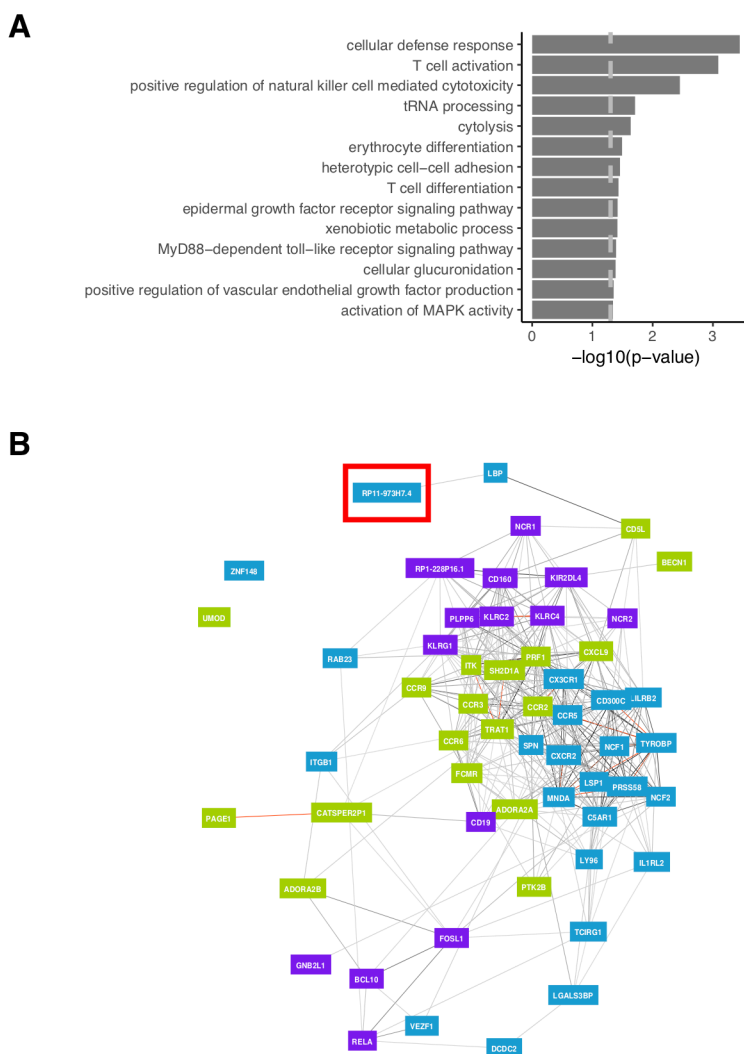
**A**



**Supplementary Fig. 5 Risk loci for autoimmune diseases are enriched in clusters of DEG responding to cytokine stimulation in IE-CTLs. (A)** The overlap between genetic risk loci associated with ten common autoimmune diseases and the transcriptional response of IE-CTLs exposed to cytokines is indicated as a percentage for each of the ten DEG clusters and disease-traits. Colors indicate significance. X-axis shows the different autoimmune diseases with their corresponding number of risk loci and total number of genes in a 250 kb window across all risk loci. Y-axis shows the number of genes present in the DEG cluster. **(B)** Empirical null distribution of a random set of genes representative for each of the DEG clusters. Blue lines indicate the observed enrichment for autoimmune risk loci within DEGs. The diseases and DEG clusters (c1-c10) are depicted on the X- and Y-axis, respectively.

**B**





**Supplementary Fig. 6 RP11-973H7.4 associated biological processes and co-expressed genes. (A)** Significant biological process (GO terms) associated with RP11-973H7.4 and co-expressed genes. **(B)** Co-expression network of genes contributing to the cellular defense response GO term from figure A, extracted from Gene Network.

